Selective oxidation of CO in excess hydrogen on copper—cerium-containing catalysts

N. Ya. Usachev, I. A. Gorevaya, E. P. Belanova, A. V. Kazakov, O. K. Atal´yan, and V. V. Kharlamov*

N. D. Zelinsky Institute of Organic Chemistry, Russian Academy of Sciences, 47 Leninsky prosp., 119991 Moscow, Russian Federation. Fax: +7 (095) 135 5328. E-mail: ny@ioc.ac.ru

Selective oxidation of CO that is in mixtures enriched in H_2 was studied to investigate catalytic properties of the 0.5—80% $CuO/Ce_{0.7}Zr_{0.3}O_2$ system. The catalysts were prepared by the combined decomposition of copper, cerium, and zirconyl nitrates at 300 °C. The systems studied are active and stable under mild conditions of the process (80—160 °C) and at high space velocities (to 100000 h^{-1}) of the reaction mixture (2% CO, 1% O_2, 40—50% H_2). With an increase in the CuO content in the catalysts up to 20%, the degree of CO removal achieves 60% (120 °C and V = 35000 h^{-1}) and further does not change appreciably. The contribution of oxygen participation into CO oxidation is virtually independent of the copper concentration in the sample and ranges from 65 to 75%. The dependences of the Arrhenius equation parameters for CO and H_2 oxidation on the catalyst composition were determined, which makes it possible to calculate the conversion of reactants and selectivity of CO conversion under the specified conditions of the process. The addition of CO_2 and H_2O (12—15%) to the reaction mixture decreases the catalyst activity and simultaneously increases the selectivity of CO oxidation to 100%. It is shown by the TPR and X-ray diffraction methods that the combined decomposition of the starting Cu^{2+}, Ce^{3+}, and ZrO^{2+} nitrates produces solid solutions of oxides with a high content of CuO. The reductive pre-treatment of fresh samples of the studied catalysts results in the destruction of the solid solution and formation of highly dispersed Cu particles on the surface of Ce—Zr—O. These particles are active in CO oxidation.

Key words: oxidation; carbon monoxide; mixed copper, cerium, and zirconium oxides; kinetics; TPR method; X-ray diffraction analysis.

Recently, researchers are intensely searching for efficient methods for preparation of high-purity hydrogen, which is necessary for operation of low-temperature fuel elements.[1] When hydrogen is obtained, *e.g.*, by steam methanol reforming, a considerable amount of CO is formed (up to 1 vol.%).[2] Meanwhile, CO is a known poison for Pt electrodes[3] and the admissible concentration of CO in hydrogen should not exceed 10^{-2} vol.%.[4] Oxidation is one of the promising methods for decreasing the CO content in hydrogen-containing mixtures. Catalysts containing noble metals (Au, Pt, Ru, Pd)[5—9] and copper[10,11] on various porous supports (carbon materials, zeolites, metal oxides) manifest high selectivity and activity in this process.

Copper catalysts on Ce-containing supports are of the greatest interest from the practical point of view. It is shown[12,13] that Cu/CeO_2 is highly active in CO oxidation with oxygen (1% CO + 0.5% O_2 + N_2) under the mild conditions: at room temperature the CO conversion is 20%, while at 125 °C it achieves 100%. The activity of this catalyst is much higher than that of Cu/Al_2O_3.[14] An important feature of cerium oxide is its ability to form solid solutions with other oxides, for example, with ZrO_2,[15—17] and in this way to increase mobility of lattice oxygen atoms and improve the redox characteristics of mixed oxides. Due to these features, the modified cerium-containing systems are promising for use as catalysts of CO oxidation in excess hydrogen. In this work, we studied the selectivity and stability of the $CuO/Ce_{0.7}Zr_{0.3}O_2$ catalysts prepared by the combined decomposition of Cu^{2+}, Ce^{3+}, and ZrO^{2+} nitrates. Catalysts with this composition were not earlier studied in the combined oxidation of CO and H_2. The catalytic properties of the systems were compared with their redox and microstructural characteristics obtained by the method of temperature-programmed reduction (TPR) and X-ray diffraction analysis.

Experimental

The (0.5—80.0%)$CuO/Ce_{0.7}Zr_{0.3}O_2$ catalysts were prepared from Cu, Ce, and ZrO nitrates by combined decomposition. Mixtures of aqueous solutions of nitrates were evaporated, dried for 1 h at 100—120 °C, and calcined in air at 300 °C for 2 h. The CuO content ([CuO]) in the $Ce_{0.7}Zr_{0.3}O_2$-based samples was

Published in Russian in *Izvestiya Akademii Nauk. Seriya Khimicheskaya,* No. 3, pp. 512—520, March, 2004.

1066-5285/04/5303-0538

0.5—80.0 wt.%. Catalytic experiments were conducted at an atmospheric pressure in a flow-type microreactor (internal diameter 6 mm). A mixture consisting of 0.025—0.05 g of the catalyst powder and 0.05 g of the quartz pellets (0.1—0.3 mm) was loaded into the reactor. The reaction mixture had the following composition (vol.%): CO, 2; O_2, 1; N_2 (internal standard), 4; H_2, 46; He, 47. In several cases, CO_2 and H_2O vapor were introduced into the reaction mixture. The space velocity was varied from 10^4 to 10^5 h^{-1}. The reactor was heated with a rate of 2 deg min^{-1}. The heating was interrupted every 20 °C for an interval of 30 min. During this time, two test samples of a rection mixture were taken for analysis. The temperature was increased to the value corresponding to the maximum conversion of O_2, and then the reactor was cooled in a similar temperature regime. Experiments were carried out at 80—280 °C. Under these conditions, conversions of O_2 and CO changed from 0 to 98—99% and from 0 to 80%, respectively. To calculate the rate constants of CO and H_2 oxidation, the descending branches of curves of the temperature plots of the carbon oxide and hydrogen conversion were used.

$$2\,CO + O_2 \xrightarrow{k_1} 2\,CO_2$$

$$2\,H_2 + O_2 \xrightarrow{k_2} 2\,H_2O$$

Reaction products were analyzed on a gas chromatograph with a heat-conductivity detector (column 3 mm × 50 cm with zeolite CaA). The conversions of oxygen ($K(O_2)$) and CO (K(CO)) were calculated by the formulas

$$K(O_2) = 100\%[(P_{O_2}/P_{N_2})_0 - (P_{O_2}/P_{N_2})_i]/(P_{O_2}/P_{N_2})_0,$$

where $(P_{O_2}/P_{N_2})_0$ and $(P_{O_2}/P_{N_2})_i$ are the ratios of surface areas of the O_2 and N_2 peaks in the initial mixture and reaction products, respectively;

$$K(CO) = 100\%[(P_{CO}/P_{N_2})_0 - (P_{CO}/P_{N_2})_i]/(P_{CO}/P_{N_2})_0,$$

where $(P_{CO}/P_{N_2})_0$ and $(P_{CO}/P_{N_2})_i$ are the ratios of surface areas of the CO and N_2 peaks in the initial mixture and reaction products, respectively.

The selectivity of CO oxidation (S(CO) is the fraction of O_2 involved in CO oxidation) was calculated from the relationship

$$S(CO) = 100\%K(CO)/K(O_2).$$

The rate constants of CO (k_1) and H_2 (k_2) oxidation were calculated by the formulas obtained by the integration of differential equations for bimolecular parallel reactions with one common component (O_2)

$$k_1 = \frac{1}{2}\frac{100}{\left(\frac{[H_2]+[CO]}{2} - [O_2]\right)t}\ln\frac{[O_2]\left(\frac{[H_2]+[CO]}{2} - x\right)}{\frac{[H_2]+[CO]}{2}([O_2]-x)} \cdot$$

$$\cdot\left(1 - \frac{1}{1 + \frac{\ln\{1-2x_1/[CO]\}}{\ln\{1-2(x-x_1)/[H_2]\}}}\right), \qquad (1)$$

$$k_2 = \frac{\frac{1}{2}\frac{100}{\left(\frac{[H_2]+[CO]}{2} - [O_2]\right)t}\ln\frac{[O_2]\left(\frac{[H_2]+[CO]}{2} - x\right)}{\frac{[H_2]+[CO]}{2}([O_2]-x)}}{1 + \frac{\ln\{1-2x_1/[CO]\}}{\ln\{1-2(x-x_1)/[H_2]\}}} \qquad (2),$$

where $[H_2]$, [CO], and $[O_2]$ are the concentrations of the respective components in the initial mixture (vol.%); x and x_1 are the amounts of reacted O_2 and CO, respectively (vol.%); t is the contact time (ratio of the catalyst weight (g) to the flow rate of the reaction mixture (mol h^{-1})).

The activation energies (E) and logarithms of pre-exponential factors ($\ln k_0$) were calculated by the Arrhenius equation using the least-squares method. The average values of the standard deviation of the Arrhenius equation parameters for CO and H_2 oxidation were ±8 and 16 rel.%, respectively.

The temperature-programmed reduction of the catalysts (20 mg of powder + 20 mg of quartz pellets) was conducted in a flow of the 10% H_2 + 90% Ar mixture (30 mL min^{-1}) in a quartz reactor (internal diameter 5 mm) with the temperature increase from 25 to 350 °C with a rate of 20 °C min^{-1}. At the moment of maximum hydrogen consumption, its conversion did not exceed 15%. Then the sample was cooled in an argon flow to a specified temperature and oxidized with air (30 mL min^{-1}) for 0.2—60 min, and the repeated reduction was carried out. The H_2—Ar mixture and argon used were purified at the reactor inlet to remove oxygen and water traces by successive passing the gases through columns packed with metallic copper, zeolite, and the Mn catalyst. Water formed due to catalyst reduction was collected in a cooled trap placed behind the reactor. A change in the hydrogen concentration in argon was detected by a katharometer.

X-ray diffraction analysis was carried out on a DRON-3M X-ray diffractometer (CuK_α radiation, nickel filter) with a scan rate of 1 deg min^{-1} in a 2θ angle interval of 5—75°. X-ray diffraction data were obtained from the spectra processed by the Rietveld method using the RIETAN-2000 program.[18] Particle size was estimated from the half-widths of the (111) peak for the $Ce_xZr_{1-x}O_2$ phase and (002) peak for the CuO phase.

Results and Discussion

The temperature plots of the oxygen and CO conversions on the 0.5%CuO/$Ce_{0.7}Zr_{0.3}O_2$ catalyst in the series of successive experimental runs are presented in Fig. 1. In this case, an experimental run is the following procedure. The temperature was raised until the highest conversion was achieved and then decreased until the reaction terminates. When the temperature increases to 280 °C, $K(O_2)$ and K(CO) over the starting sample achieve 99 and 55%, respectively (see Fig. 1, *a*, curves *1* and *2*). The subsequent temperature decrease decreases the conversion of the reactants. However, the curve of the temperature plot of the conversion lies above the respective curve obtained by the temperature increase, *i.e.*, hysteresis of the catalytic activity is observed. In the repeated run (the catalyst

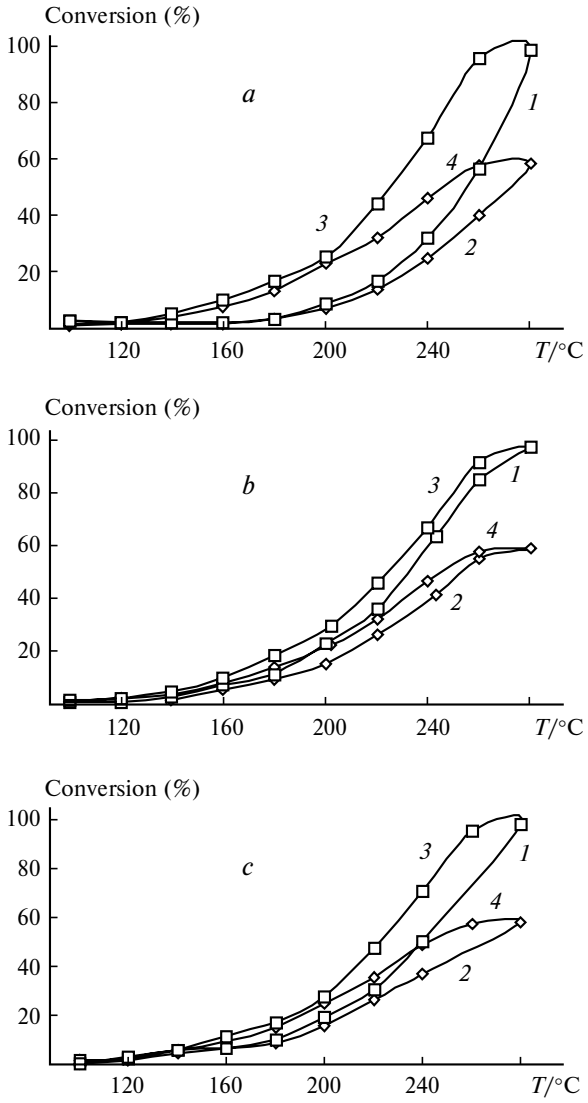

Fig. 1. Change in the conversions of O_2 (*1*, *3*) and CO (*2*, *4*) on heating (*1*, *2*) and cooling (*3*, *4*) the 0.5%$CuO/Ce_{0.7}Zr_{0.3}O_2$ catalyst: *a*, experiment with the fresh sample; *b*, repeated run (after the catalyst was cooled in the reaction mixture to 60 °C); *c*, run after runs *a* and *b* and additional treatment of the catalyst at 300 °C in an air flow for 1 h.

did not contact with O_2), the character of the temperature dependences of $K(O_2)$ and K(CO) remains unchanged but the width of the hysteresis loop became much narrower (see Fig. 1, *b*). After the oxidative treatment of the catalyst (300 °C, 1 h), the hysteresis phenomenon becomes more visible (see Fig. 1, *c*), although does not achieve the level observed for the fresh catalyst (see Fig. 1, *a*).

Note that the hysteresis phenomenon for the catalytic activity is characteristic of oxidation reactions and is widely discussed in literature. When CO was oxidized in the H_2—O_2—CO (97 : 2 : 1, vol.%) mixture on the 5%$CuO/Ce(Sm)O_2$ catalyst prepared by the impregnation of the mixed oxide with a solution of $Cu(NO_3)_2$, the same conversions of CO were achieved at higher temperatures on cooling than on heating.[11] The hysteresis phenomenon was observed[19] for CO oxidation (the mixture contained no hydrogen, and Ar—O_2—CO = 95 : 3 : 2 vol.%) on the 0.6 and 1.5% $Cu/Zr(Y)O_2$ catalysts. In this system active sites are believed to be formed at the interface of the oxide phases and represent oxygen vacancies in the ZrO_2 lattice stabilized by the Y_2O_3 additive near which the Cu^+ cations are located.[19] Due to CO oxidation, the active sites become "hot" and retain an enhanced activity in the initial period of cooling.

It is difficult to accept a similar assumption for the explanation of hysteresis of the $CuO/Ce_{0.7}Zr_{0.3}O_2$ sample prepared by the combined decomposition of the starting salts. The sizes of hysteresis loops differ substantially in experiments with the fresh catalyst and samples treated with a hydrogen-containing mixture or air (see Fig. 1). This indicates that the processes of catalyst reduction resulting in the formation of active sites contribute noticeably to the relative increase in the catalyst activity.

The catalyst activity in CO oxidation increases with an increase in the CuO content in the catalysts (Fig. 2). Hereinafter we present the results for the catalysts obtained for descending branch of the hysteresis loop. The maximum changes in $K(O_2)$ and K(CO) (to 70 and 50%, respectively) are observed in the interval of CuO concentrations from 0.5 to 7.5%. In the presence of the 20%$CuO/Ce_{0.7}Zr_{0.3}O_2$ sample, K(CO) exceeds 60%. On going to the samples with 50 and 80% CuO, no noticeable increase is observed in the activity of the $CuO/Ce_{0.7}Zr_{0.3}O_2$ in CO oxidation, although the total conversion of O_2 approaches 100% due to oxygen consumption in the oxidation of H_2. Note that some authors[20,21] found an increase in the activity of the

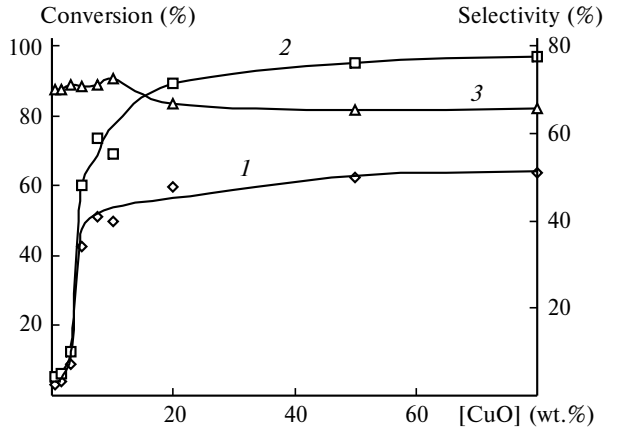

Fig. 2. Conversions of CO (*1*) and O_2 (*2*) and the selectivity of CO oxidation (*3*) *vs.* CuO content in the $CuO/Ce_{0.7}Zr_{0.3}O_2$ catalyst at 120 °C and $V = 35000\ h^{-1}$.

CuO/CeO_2 systems (prepared by impregnation) in CO oxidation (2.4% CO + 1.2% O_2 + 96.4% N_2) with an increase in [CuO] to 3—5%. Probably, the difference between the dependence of K(CO) on [CuO] obtained in the present and other works[20,21] is caused by specific features of methods for preparation of the catalysts, their chemical compositions, and conditions of CO oxidation. The S(CO) value for the 0.5—10%$CuO/Ce_{0.7}Zr_{0.3}O_2$ catalysts is higher than 70% at 120 °C and 35000 h^{-1}. This can indicate that active sites of similar nature are formed in this interval of CuO concentrations, and the ratio of the rates of CO and H_2 oxidation on these active sites remains unchanged. For the catalysts with [CuO] >10%, the increase in activity in CO oxidation slows down, although $K(O_2)$ increases from 70 to 97%, which results in some decrease in S(CO) (to 65%).

The 5%$CuO/Ce_{0.7}Zr_{0.3}O_2$ catalyst was studied over wide range of temperatures and space velocities. An increase in the space velocity resulted in a regular decrease in the conversions of oxygen and CO (Fig. 3, *a* and *b*). In this series of experiments, the space velocity was changed by varying both the flow rate of the starting substances (8.3—41.7 mL min^{-1}) and the catalyst sample weight (25—50 mg). The result was independent of the method by which this space velocity was achieved, indicating the absence of external diffusion control. Since the catalysts were used as powders, we can assume that internal diffusion does not affect the kinetics of the process as well. The values of the experimental and calculated conversions (see Fig. 3) are close: the error on the average did not exceed 20 rel.%. This indicates that the kinetic equations used are adequate to the experimental data.

The variation of the CuO concentrations in the catalysts also changes the activation energies and pre-exponential factors. The activation energy of CO oxidation changes from 13.7 to 23.2 kcal mol^{-1}, and the sharpest increase in E_1 (from 13.7 to 18.0 kcal mol^{-1}) is observed in an interval of 0.5—7.5% CuO (Fig. 4, *a*). The obtained E_1 values are close to the published data (17—23 kcal mol^{-1}) for the Cu-containing catalysts (Cu/Ce(La)O [22] and $Cu/\delta\text{-}Al_2O_3$ [23]). The pattern of dependence of the pre-exponential factor on the rate constant of CO oxidation is similar to the E_1—[CuO] profile: the maximum increase in $\ln k_{01}$ (from 15.8 to 25.0) is observed for the catalysts containing 0.5—7.5% CuO. Since K(CO) mainly increases in the same interval of CuO concentrations (see Fig. 2), we can assume that the increase in the catalyst activity is related to an increase in the number of active sites.

The dependence of the Arrhenius equation parameters for hydrogen oxidation (see Fig. 4, *b*) on the CuO content passes through a smooth maximum at a concentration of 20% CuO in the catalyst (E_2 = 20.6 kcal mol^{-1}, $\ln k_{02}$ = 23.6). The differences revealed in the character of the dependences of E and $\ln k_0$ on [CuO] in the reactions under study reflect an increase in the fraction of O_2 in-

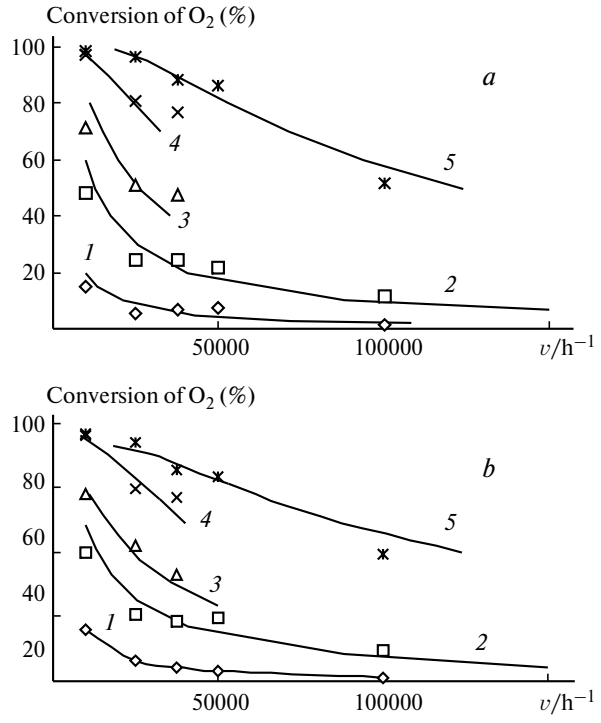

Fig. 3. Conversions of O_2 (*a*) and CO (*b*) *vs.* space velocity (points are experimental data, curves are calculated from the reaction rate constants by Eqs (1) and (2)) on the 5%$CuO/Ce_{0.7}Zr_{0.3}O_2$ catalyst at 75 (*1*), 100 (*2*), 110 (*3*), 120 (*4*), and 125 °C (*5*).

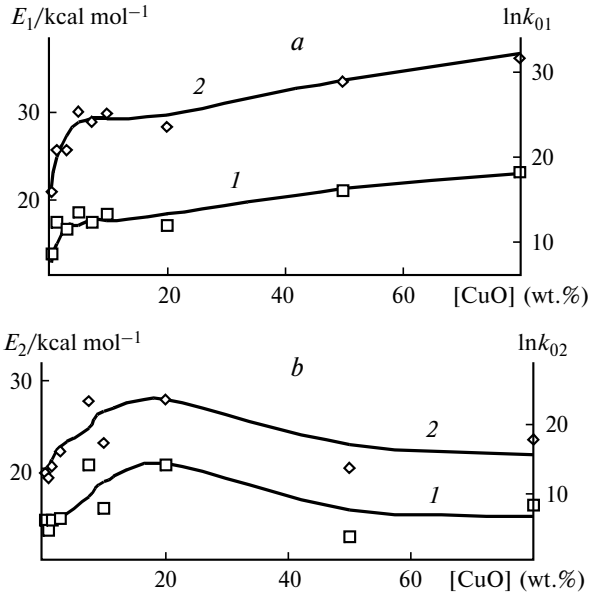

Fig. 4. Activation energy (*1*) and the logarithm of the pre-exponential factor of the rate constant (*2*) in the oxidation of CO (*a*) and H_2 (*b*) *vs.* CuO content in the $CuO/Ce_{0.7}Zr_{0.3}O_2$ catalysts. Reaction conditions: 60—240 °C, V = 35000 h^{-1}.

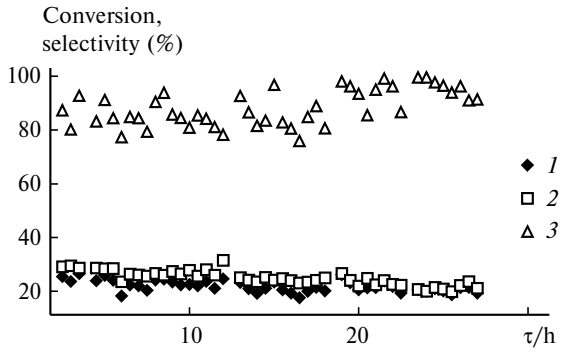

Fig. 5. Conversions of CO (*1*) and O_2 (*2*) and the selectivity of CO oxidation (*3*) *vs.* time of stream on the 5%CuO/$Ce_{0.7}Zr_{0.3}O_2$ catalyst at 100 °C and $V = 25000\ h^{-1}$.

volved in H_2 oxidation at high copper concentrations in the catalyst (see Fig. 2). The dependences of the parameters of the Arrhenius equation on the composition of the catalytic systems found for the oxidation of CO and H_2 in the temperature interval from 60 to 240 °C make it possible to calculate the expected conversions of the reactants and selectivity of CO transformation under the specified conditions of the process (*T*, space velocity, and ratio of components of the reaction mixture).

The CuO/$Ce_{0.7}Zr_{0.3}O_2$ systems manifest favorable time-on-stream catalyst behavior (Fig. 5). These tests were carried out at 100 °C when conversions of the reactants were relatively low, and determination of variations in the catalyst activity are more reliable. No appreciable decrease in the CO and O_2 conversions was observed for 28 h: K(CO) and $K(O_2)$ were at a level of 20—25%; the selectivity of oxygen participation in CO oxidation being higher than 70%. The high stability of the Cu-containing catalyst based on CeO_2 was observed[10] for the transformation of the 1% CO/1.25% O_2/50% H_2 mixture at 140 °C.

Real hydrogen-containing mixtures obtained by steam conversion of hydrocarbons and alcohols contain, as a rule, H_2O and CO_2. Therefore, we studied the influence of these components on the activity of the CuO/$Ce_{0.7}Zr_{0.3}O_2$ catalysts. The replacement of a portion of helium in the reaction mixture by CO_2 (12 vol.%) decreases $K(O_2)$ values from 96.2 to 74.9, whereas the selectivity of CO oxidation increases from 74.7 to 100% (Table 1). When CO_2 and H_2O are simultaneously introduced into the reaction mixture, the conversion of O_2 decreases to 39.2% but the 100% selectivity with respect to CO is retained. The changes occurred in the catalyst activity can be monitored by a decrease in the rate constants of CO and H_2 oxidation. In the initial mixture, k_1 (15.5 mol g^{-1} h^{-1} atm^{-2}) substantially exceeds k_2 (0.13 mol g^{-1} h^{-1} atm^{-2}). In mixtures containing CO_2 and CO_2+H_2O in which H_2 is not oxidized ($k_2 = 0$), k_1 decreased two- and sixfold, respectively. These data indicate that the active sites of the Cu—Ce—Zr—O system are blocked by CO_2 and H_2O molecules. The deactivation effect of these compounds appears, first of all, in the oxidation of H_2, indicating, most likely, that CO and H_2 are oxidized on different active sites. The inhibition effect of CO_2 and H_2O on CO oxidation was also observed for the CuO—CeO_2 catalyst[10] and systems containing Pt, Pd, and Ru.[7]

Let us compare the catalytic properties of the Cu-containing systems in CO oxidation in excess hydrogen using the rate constants of CO and H_2 oxidation, which were calculated by Eqs (1) and (2). Table 2 contains our

Table 1. Influence of CO_2 and H_2O on the kinetics of CO oxidation in the presence of H_2 on the 5%CuO/$Ce_{0.7}Zr_{0.3}O_2$ catalyst at 150 °C, $V = 50000\ h^{-1}$

Composition of gas mixture (vol.%)							$K(O_2)$	K(CO)	S(CO)	k_1	k_2
CO	O_2	N_2	H_2	CO_2	He	H_2O	(%)			mol g^{-1} h^{-1} atm^{-2}	
2	1	4	46	—	47	—	96.2	71.9	74.7	15.5	0.13
2	1	4	50	12	31	—	74.9	74.8	100	6.5	0
2	1	4	50	12	16	15	39.2	39.1	100	2.3	0

Table 2. Comparison of the properties of the Cu-containing catalysts in selective CO oxidation

Run	Catalyst	Conditions of process*						K(CO)	S(CO)	k_1	k_2	Ref.
		v/h^{-1}	Composition (vol.%)					(%)		mol g^{-1} h^{-1} atm^{-2}		
			CO	O_2	H_2	He	N_2					
1	5.7% CuO/CeO_2	120000	1	1.25	50	47.75	—	88	93	5.3	$5.2 \cdot 10^{-3}$	10
2	5%CuO/$Ce_{0.9}Sm_{0.1}O_2$	150000	1	2	97	—	—	90	26	13.2	0.2	11
3	7.5%CuO/$Ce_{0.7}Zr_{0.3}O_2$	35000	2	1	46	47	4	67	67	15.1	0.2	**

* $T = 140$ °C. ** Data of this work.

results and the most reliable published data on the Cu-containing catalysts obtained by the oxidation of CO in hydrogen excess.[10,11] These experiments were carried out with the reaction mixtures containing a stoichiometric excess of O_2 relatively to CO (2.5 and 4). The 90% conversion of CO was achieved in the presence of 5.7%CuO/CeO_2 and 5%$CuO/Ce_{0.9}Sm_{0.1}O_2$. The results obtained on the 5%$CuO/Ce_{0.9}Sm_{0.1}O_2$ catalyst[11] are comparable with our data.

An important information on the state of the catalytic Cu—Ce—Zr—O systems was obtained by the H_2-TPR method in a series of successive reduction—oxidation (air) cycles. For the fresh 7.5%$CuO/Ce_{0.7}Zr_{0.3}O_2$ sample, the TPR curve has one peak at 180—280 °C with a maximum near 235 °C (Fig. 6). Oxidation of this sample at 300 °C shifted the onset of hydrogen consumption to a lower temperature (130 °C) to complete it at 220 °C. In addition, two maxima (at 160 and 185 °C) appear in the TPR curve. In the subsequent cycles, the shape of the TPR curves and positions of the T maxima were almost independent of the oxidation temperature in the 25—200 °C interval.

The volume of consumed H_2 (0.74 mL) for the fresh sample corresponds to $H_2/Cu = 1.9$ (Table 3). This H_2 amount is nearly twice as much as the amount of H_2 required for the reduction of CuO to Cu. This indicates that the CeZr-oxide matrix is partially reduced. A change in the state of the sample after its reduction and oxidation causes reduction of the H_2/Cu ratio to 1.0. In the subsequent experiments, the H_2/Cu ratio decreases successively and reaches a value of 0.79 after reoxidation at 25 °C. The variation of the duration of low-temperature treatment of the sample with air (from 0.2 to 20 min) insignificantly changes the degree of its oxidation: the H_2/Cu ratio varies from 0.69 to 0.76. This degree of dispersion indicates a small size of copper particles in the reduced catalyst, which favors a sufficiently high rate of

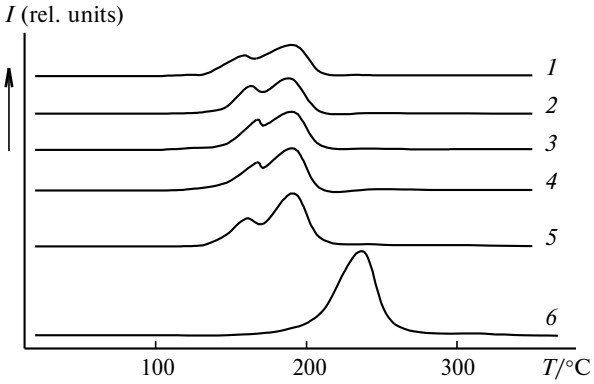

Fig. 6. Temperature-programmed reduction of the 7.5%$CuO/Ce_{0.7}Zr_{0.3}O_2$ catalyst oxidized for 1 h at different temperatures/°C: 25 (*1*), 50 (*2*), 100 (*3*), 200 (*4*), 300 (*5*), and fresh sample (*6*).

Table 3. Volumes of consumed H_2 (V) and the H_2/Cu molar ratio for the fresh 7.5%$CuO/Ce_{0.7}Zr_{0.3}O_2$ catalyst and samples repeatedly oxidized in an air flow at different temperatures

T/°C	τ/min	V/mL	H_2/Cu/mol
Fresh		0.74	1.89
300	60	0.39	1.0
200	60	0.39	1.0
100	60	0.36	0.91
50	60	0.33	0.84
25	60	0.31	0.79
25	0.2	0.27	0.69
25	1	0.28	0.71
25	2	0.30	0.76
25	20	0.30	0.76
300	60	0.38	0.97

τ is the duration of oxidation.

their oxidation. After the temperature of oxidative treatment was increased to 300 °C, the H_2/Cu ratio again achieved a level observed in the experiment after the first oxidation of the sample (see Table 3). Reversibility of the redox transitions indicates a high stability of the CuO/Ce—Zr—O system.

The results obtained for the CuO/Ce-containing support system by the TPR method are interpreted in different ways.[20,21,24—26] According to the published data,[20,21] the hydrogen reduction of the fresh 0.5—10%CuO/CeO_2 sample obtained by impregnation occurs in two steps in the 130—270 °C interval. This character of reduction is related to CuO particles with different sizes on the support surface. With an increase in the fraction of large particles, hydrogen consumption shifts toward high temperatures. A similar TPR spectrum with two maxima at 190 and 239 °C was obtained[26] for the 1.27%CuO/CeO_2 sample. The presence of two maxima is explained[26] by the stepwise change in the valent state of Cu^{2+}, which includes particular steps $Cu^{2+} \rightarrow Cu^{+}$ and $Cu^{+} \rightarrow Cu^{0}$.

The study of the $Cu_xCe_{1-x}O_2$ systems ($x = 0.1$—0.7) obtained by co-precipitation of metal hydroxides showed[24] that for the samples containing 5.7—12.8% CuO ($x = 0.2$) the TPR curves have only one peak (near 170 °C). This peak was assigned to the reduction of CuO in the $CuO—CeO_2$ solid solution. An increase in the CuO content resulted in the appearance of the second peak with a maximum at 210 °C, which shifts to the high-temperature region with the [CuO] increase. This shift was explained[24] by replenishment of all site vacancies in the cerium oxide lattice and migration of CuO to the CeO_2 surface. The authors of another work[25] found an excessive consumption of hydrogen caused, in authors´ opinion, by the reduction of the oxide surface in the 2.7—5.7%CuO—Ce(4.5 at.% La)O_2 systems, whose preparation included co-precipitation (solution of metal

nitrates + carbamide) and calcination at 650 °C. On the basis of excessive hydrogen consumption (H_2/Cu was 1.7 and 1.2, respectively), the authors concluded[15] that the presence of CuO in Ce(La)O_2 favored the reduction of the oxide matrix under mild conditions (below 200 °C), although individual CeO_2 interacts with H_2 only at temperatures higher than 500 °C.

Taking into account the published data, we can make some conclusions on the state of the 7.5%CuO/$Ce_{0.7}Zr_{0.3}O_2$ system. The combined decomposition of nitrates with thermal treatment at 350 °C results in the formation of the oxide system as a solid solution. The main part of copper cations are linked through oxygen bridges with the cerium ions (Ce^{4+}—O—Cu^{2+}—O—Ce^{4+}), and reduction affects both Cu^{2+} ions and the respective amount of Ce^{4+} ions. This is indicated by the high H_2/Cu value (1.9) determined for the fresh 7.5%CuO/$Ce_{0.7}Zr_{0.3}O_2$ sample (see Table 3). The process can be presented by the following scheme:

$$Cu^{2+}(OCe^{4+})_2 + 2\ H_2 = Cu^0 + 2\ Ce^{3+} + 2\ H_2O.$$

The 7.5%CuO/$Ce_{0.7}Zr_{0.3}O_2$ sample contains more $Cu^{2+}(OCe^{4+})_2$ fragments than the CuCe(La)O_2 [25] system with a lower content of CuO (5.7%). For this system, the H_2/Cu ratio was only 1.2. The observed differences are evidently related to methods of sample preparation. The preparation of the CuO/$Ce_{0.7}Zr_{0.3}O_2$ catalysts by the thermal decomposition of a mixture of salts provides, probably, a more uniform distribution of components in this oxide system than that in the case of precipitation methods.[24,25]

The fresh 7.5%CuO/$Ce_{0.7}Zr_{0.3}O_2$ sample can be reduced (see Fig. 6) in the high-temperature region (180—280 °C). The reason is probably that the destruction of the Cu—Ce—Zr—O_2 solid solution is impeded by ion diffusion from the bulk to the oxide matrix surface. Based on this fact, we believe that the low-temperature peak in the TPR curves of the $Cu_xCe_{1-x}O_2$ samples cannot be explained completely by reduction of the solid solution.[24] When interpreting the TPR data, one has to take into account, most likely, the texture features of the samples and the character of Cu^{2+} distribution in particles of the oxide matrix, which can affect the ability of copper ions to undergo reduction. After the reduction and repeated oxidation of 7.5%CuO/$Ce_{0.7}Zr_{0.3}O_2$ (see Fig. 6), the state of this system changes, because, most likely, the main part of Cu^{2+} ions irreversibly leave the mixed CeZr oxide. The CuO oxide localized on the support surface is reduced at lower temperatures in two steps, which is characteristic of the CuO-containing systems.[20,21,26] The stepwise character of this process can be caused by both the $Cu^{2+} \rightarrow Cu^{+} \rightarrow Cu^0$ transitions[26] and the reduction of the Cu^{2+} ions contacting with the oxide matrix.[20]

An additional information on the interaction of the components in the CuO/$Ce_{0.7}Zr_{0.3}O_2$ systems was obtained by X-ray diffraction analysis. The positions of the main reflections at 28.8, 33.3, 47.9, and 56.8° (2θ) in the X-ray patterns of the fresh samples, including CeO_2 and $Ce_{0.7}Zr_{0.3}O_2$ (Fig. 7), correspond to the cubic structure of CeO_2. An increase in the CuO content to 20% does not produce reflections characteristic of the CuO structure. This can be related to both the localization of Cu^{2+} ions in a solid solution and the small size of CuO particles unidentified by X-ray diffraction method. The X-ray patterns of the samples with a high content of CuO (50 and 80%) exhibit peaks at 35.4 and 38.8° (2θ), indicating the formation of the monoclinic CuO phase. Their intensities increase regularly on going from 50%CuO/$Ce_{0.7}Zr_{0.3}O_2$ to the sample with 80% copper oxide. The peaks from the CuO phase are not observed in the X-ray patterns of the 20%CuO/$Ce_{0.7}Zr_{0.3}O_2$ sample treated with hydrogen (300 °C, 0.5 h) and then oxidized (air, 25 °C). This indicates the formation of a highly dispersed CuO phase undetected by the X-ray diffraction method.

The microstructural characteristics of the samples under study are presented in Table 4. The cell parameter (a) of individual CeO_2 is 0.5425 nm, which corresponds to the published data.[27,28] In the case of $Ce_{0.7}Zr_{0.3}O_2$, the cell parameter decreases to 0.5403 nm. This indicates that Zr^{4+} ions with a smaller size (0.086 nm) are incorporated into the CeO_2 lattice (ion radius of Ce^{4+} 0.102 nm), which agrees with known data[16,17,28] for the Ce—Zr—O systems. A change in the cell parameter of $Ce_xZr_{1-x}O_2$ depends, to a great extent, on the method of preparation and the calcination temperature of the samples.[29] The oxide obtained by the decomposition of Ce nitrate at 300 °C occurs as particles with a mean size of 9.5 nm. At the same time, the formation of mixed oxide $Ce_{0.7}Zr_{0.3}O_2$ results in the formation of particles with a smaller size (~7.5 nm).

Table 4. Microstructural characteristics of the CuO/$Ce_{0.7}Zr_{0.3}O_2$ catalysts according to the X-ray diffraction data

Sample	[CuO] (%)	a* /nm	Particle size /nm	
			$Ce_xZr_{1-x}O_2$	CuO
CeO_2	—	0.5425	9.5	—
$Ce_{0.7}Zr_{0.3}O_2$	—	0.5403	7.6	—
CuO	100	—	—	39.4
5%CuO/$Ce_{0.7}Zr_{0.3}O_2$	0	0.5397	6.3	—
10%CuO/$Ce_{0.7}Zr_{0.3}O_2$	0	0.5398	5.6	—
20%CuO/$Ce_{0.7}Zr_{0.3}O_2$	0	0.5375	4.8	—
20%CuO/$Ce_{0.7}Zr_{0.3}O_2$**	0	0.5371	5.8	—
50%CuO/$Ce_{0.7}Zr_{0.3}O_2$	16.1	0.5370	3.8	20.1
80%CuO/$Ce_{0.7}Zr_{0.3}O_2$	50.6	0.5366	4.2	24.9

* Cell parameter.
** H_2, 300 °C; air, 20 °C.

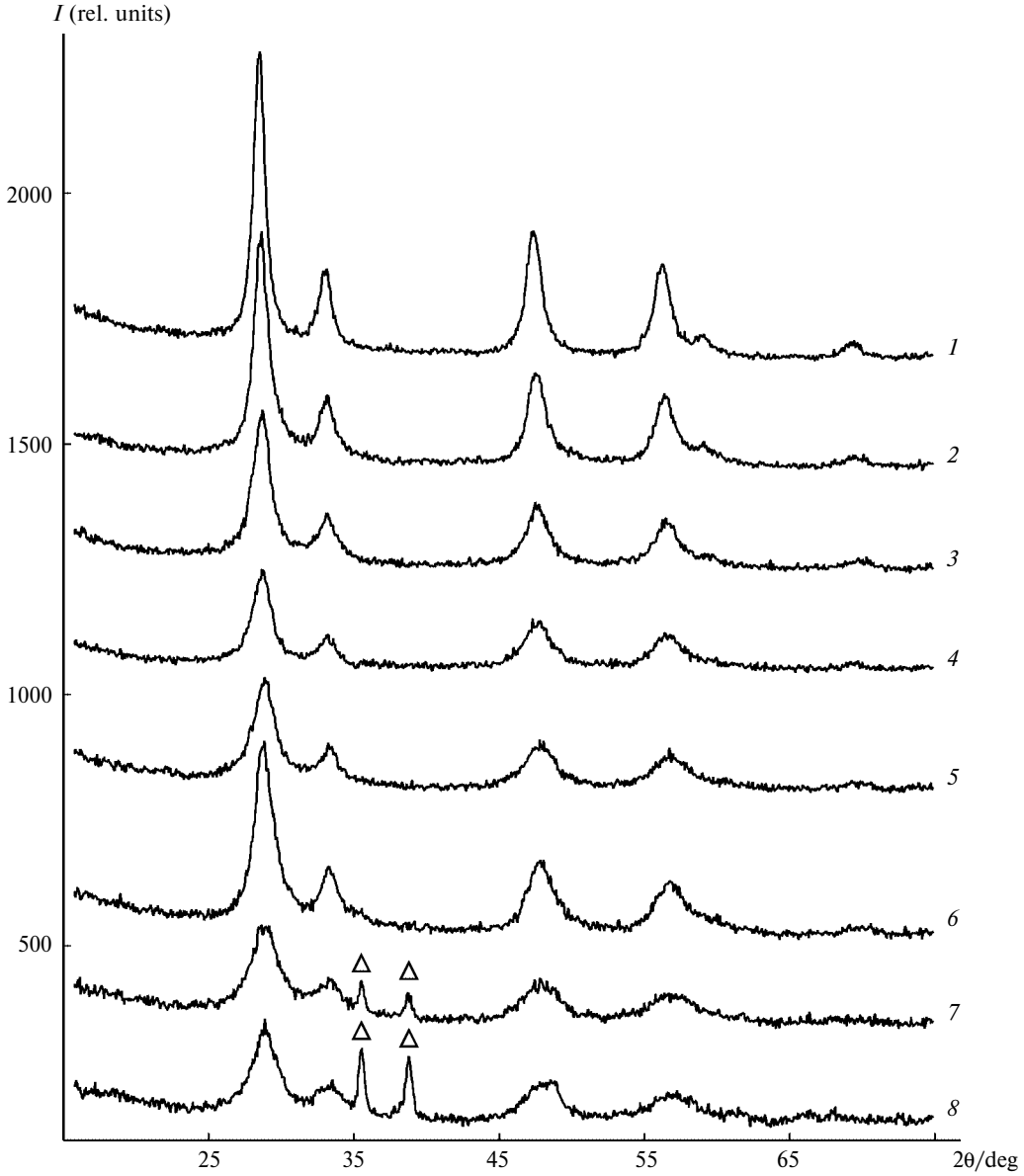

Fig. 7. X-ray diffraction patterns of the $CuO/Ce_{0.7}Zr_{0.3}O_2$ samples with different concentrations of copper oxide (calcination for 2 h at 300 °C): CeO_2 (*1*), $Ce_{0.7}Zr_{0.3}O_2$ (*2*), 5%$CuO/Ce_{0.7}Zr_{0.3}O_2$ (*3*), 10%$CuO/Ce_{0.7}Zr_{0.3}O_2$ (*4*), 20%$CuO/Ce_{0.7}Zr_{0.3}O_2$ (*5*), 20%$CuO/Ce_{0.7}Zr_{0.3}O_2$ (H_2, 300 °C) (*6*), 50%$CuO/Ce_{0.7}Zr_{0.3}O_2$ (*7*), and 80%$CuO/Ce_{0.7}Zr_{0.3}O_2$ (*8*).

When the Zr content increases from 20 to 50 mol.% in the $Ce_xZr_{1-x}O_2$ samples prepared by co-precipitation of the oxides in the presence of a surfactant $C_{14}H_{29}N(CH_3)_3Br$ and calcined at 200 °C, the size of crystals of the oxide system decreases from 9.0 to 6.0 nm. The authors[17] believe that the ZrO_2 additive inhibits the growth of mixed oxide particles.

On introducing CuO (ion radius of Cu^{2+} 0.079 nm) into the $Ce_{0.7}Zr_{0.3}O_2$ oxide matrix, its cell parameter decreases (see Table 4). This indicates that some Cu^{2+} ions are incorporated into the structure of mixed oxide. The formation of a solid solution was also observed for the CuO/CeO_2 system[21] in which the cell parameter of CeO_2 decreased with an increase in [CuO] to 15%. On going from $Ce_{0.7}Zr_{0.3}O_2$ to the 5—80%$CuO/Ce_{0.7}Zr_{0.3}O_2$ systems (see Table 4), the incorporation of CuO also decreases the size of oxide matrix particles from 7.5 to ~4 nm, which indicates a noticeable influence of the ratio of starting salts on the texture of the mixed oxides formed. It is most likely that the thermolysis of salts results in the formation of particles of both the solid solution and copper oxide. An increase in the copper oxide content impedes agglomeration of mixed oxide particles. This influence is mutual, which is indicated by an almost twofold

decrease in the CuO particle size in the samples with 50 and 80% CuO (20—25 nm) compared to a similar parameter of individual copper oxide (40 nm).

In the $50\%CuO/Ce_{0.7}Zr_{0.3}O_2$ and $80\%CuO/Ce_{0.7}Zr_{0.3}O_2$ systems, the CuO content calculated by the X-ray diffraction data is much lower than the real values: 16.1 and 50.6%, respectively (see Table 4). Similar discrepancies were observed[20] for the $5—15\%CuO/CeO_2$ impregnation systems in which 62—77% CuO were detected by X-ray diffraction analysis. Comparison of these results show that the method of combined decomposition of starting nitrates gives more dispersed systems. They contain only X-ray amorphous copper oxide at [CuO] lower than 20%, and even the $50\%CuO/Ce_{0.7}Zr_{0.3}O_2$ sample exhibits only ~30% of the incorporated amount of CuO.

Thus, the combined decomposition of the starting salts creates favorable conditions for the formation of a solid solution of metal oxides containing considerable amounts of CuO (to 10%). The reduction of copper ions in a solid solution is impeded, which is a reason for broad loops of temperature hysteresis of the activity of fresh samples. The destruction of a solid solution produces highly dispersed Cu particles on the Ce—Zr—O support surface. They are the centers of selective oxidation of CO. Their concentration increases almost proportionally as the [Cu] increases up to 10%. At [Cu] >10%, an increase in the activity of the catalyst in CO oxidation slows down due to the formation of larger Cu particles. This decreases the fraction of surface copper atoms, prevents their contact with the Ce—Zr matrix, and impedes redox transitions in the Cu—Ce—Zr—O system. Some decrease in the selectivity of the process is probably caused by the presence of large Cu particles in the catalysts with [Cu] >10%. The high activity, selectivity, and stability of the catalysts in carbon monoxide removal from the hydrogen-containing mixtures are achieved at the optimum copper content in the Cu—Ce—Zr—O systems prepared by the combined decomposition of the starting salts.

References

1. R. A. Lemons, *J. Power Sources*, 1990, **29**, 251.
2. B. Lindstrom, L. J. Pettersson, and P. G. Menon, *Appl. Catal. A: Gen.*, 2002, **234**, 111.
3. S. Gottesfeld and J. Pafford, *J. Electrochem. Soc.*, 1988, **135**, 2651.
4. R. Kumar and S. Ahmed, *Fuels Processing for Transportation Fuel Cell Systems, Presented at the First International Symposium on New Materials for Fuel Cell Systems*, Montreal, Canada, July 1995, 224.
5. S. H. Oh and R. M. Sinkevitch, *J. Catal.*, 1993, **142**, 254.
6. H. Igarashi, H. Uchida, M. Suzuki, Y. Sasaki, and M. Watanabe, *Appl. Catal. A: Gen.*, 1997, **159**, 159.
7. P. V. Snytnikov, V. A. Sobyanin, V. D. Belyaev, P. G. Tsyrulnikov, N. B. Shitova, and D. A. Shlyapin, *Appl. Catal. A: Gen.*, 2003, **239**, 149.
8. G. K. Bethke and H. H. Kung, *Appl. Catal. A: Gen.*, 2000, **194—195**, 43.
9. M. M. Schubert, V. Plzak, J. Garche, and R. J. Behm, *Catal. Lett.*, 2001, **76**, 143.
10. G. Avgouropoulos, T. Ioannides, H. K. Matralis, J. Batista, and S. Hocevar, *Catal. Lett.*, 2001, **73**, 33.
11. J. B. Wang, S.-C. Lin, and T.-J. Huang, *Appl. Catal. A: Gen.*, 2002, **232**, 107.
12. A. Martínez-Arias, J. Soria, R. Cataluña, and J. C. Conesa, *V. Cortés Corberán, Stud. Surf. Sci. Catal.*, 1998, **116**, 591.
13. A. Martínez-Arias, M. Fernández-García, J. Soria, and J. C. Conesa, *J. Catal.*, 1999, **182**, 367.
14. P. W. Park and J. S. Ledford, *Catal. Lett.*, 1998, **50**, 41.
15. P. Fornasiero, G. Balducci, R. D. Monte, J. Kašpar, V. Sergo, G. Gubitosa, A. Ferrero, and M. Graziani, *J. Catal.*, 1996, **164**, 173.
16. T. Nakatani and H. Okamoto, *J. Sol-Gel Sci. Technol.*, 2003, **26**, 859.
17. J. A. Wang, M. A. Valenzuela, S. Castillo, J. Salmones, and M. Moran-Pineda, *J. Sol-Gel Sci. Technol.*, 2003, **26**, 879.
18. F. Izumi and T. Ikeda, *Mater. Sci. Forum*, 2000, **198**, 321.
19. W.-P. Dow and T.-J. Huang, *J. Catal.*, 1996, **160**, 171.
20. M. F. Luo, Y.-J. Zhong, X.-X. Yuan, and X.-M. Zheng, *Appl. Catal. A: Gen.*, 1997, **162**, 121.
21. X. Jiang, G. Lu, R. Zhou, J. Mao, Y. Chen, and X. Zheng, *Appl. Surf. Sci.*, 2001, **173**, 208.
22. W. Liu, A. F. Sarofim, and M. Flytzani-Stephanopoulos, *Chem. Eng. Sci.*, 1994, **49**, 4871.
23. K. I. Choi and M. A. Vannice, *J. Catal.*, 1991, **131**, 22.
24. Y. Liu, T. Hayakawa, K. Suzuki, S. Hamakawa, T. Tsunoda, T. Ishii, and M. Kumagai, *Appl. Catal. A: Gen.*, 2002, **223**, 137.
25. Lj. Kundakovic and M. Flytzani-Stephanopoulos, *Appl. Catal. A: Gen.*, 1998, **171**, 13.
26. Y. Hu, L. Dong, J. Wang, W. Ding, and Y. Chen, *J. Mol. Catal. A: Chem.*, 2000, **162**, 307.
27. W. Wang, P. Lin, Y. Fu, and G. Cao, *Catal. Lett.*, 2002, **82**, 19.
28. S. Pengpanich, V. Meeyoo, T. Rirksomboon, and K. Bunyakiat, *Appl. Catal. A: Gen.*, 2002, **234**, 221.
29. S. Rossignol, F. Gérard, D. Duprez, *J. Mater. Chem.*, 1999, **9**, 1615.

Received December 30, 2003;
in revised form February 11, 2004